

RESEARCH ARTICLE

Deep Learning to Predicting Live Births and Aneuploid Miscarriages from Images of Blastocysts Combined with Maternal Age

Yasunari Miyagi^{1,2*}, Toshihiro Habara³, Rei Hirata³, and Nobuyoshi Hayashi³

¹Medical Data Labo, Okayama City, Okayama Pref, Japan.

²Department of Gynecologic Oncology, Saitama Medical University International Medical Center, Hidaka City, Saitama Pref., Japan.

³Okayama Couple's Clinic, Okayama City, Okayama Pref., Japan.

Abstract

Objectives: Making an artificial intelligence (AI) classifier that uses the maternal age and an image of the implanted blastocyst to determine the probability of getting a live birth.

Methods: The dataset comprised maternal age data and 407 images of blastocysts which led to live births and 246 images of blastocysts which led to aneuploid miscarriages, matched for maternal age. An AI system using deep learning was developed for predicting the classification and probability of a live birth.

Results: The accuracy, sensitivity, specificity, and positive and negative predictive values of the developed AI classifier were 0.75, 0.82, 0.64, 0.79, and 0.68, respectively. The area under the curve was 0.73 ± 0.04 (mean \pm standard error).

Conclusions: A classifier using AI for a blastocyst image combined with the maternal age showed potential in determining the probability of a live birth.

Key Words: Aneuploid; Live birth; Blastocyst; Artificial intelligence; Deep learning

***Corresponding Author:** Yasunari Miyagi, Visiting Professor, Department of Gynecologic Oncology, Saitama Medical University, International Medical Center, 1397-1 Yamane, Hidaka-City, Saitama Pref., Japan 350-1298; E-mail: [ymiyagi@mac.com](mailto:y Miyagi@mac.com)

Received Date: November 11, 2021, **Accepted Date:** December 15, 2021, **Published Date:** January 15, 2022

Citation: Yasunari Miyagi, Toshihiro Habara, Rei Hirata, and Nobuyoshi Hayashi. Deep Learning to Predicting Live Births and Aneuploid Miscarriages from Images of Blastocysts Combined with Maternal Age. *Int J Bioinform Intell Comput.* 2021;1(1):11-23.



This open-access article is distributed under the terms of the Creative Commons Attribution Non-Commercial License (CC BY-NC) (<http://creativecommons.org/licenses/by-nc/4.0/>), which permits reuse, distribution and reproduction of the article, provided that the original work is properly cited, and the reuse is restricted to non-commercial purposes.

1. Introduction

Assuring a live birth without chromosomal abnormality might be the optimal aim in assisted reproductive technology. Miscarriage and development failure of embryo are costly and result in lost time. Moreover, it is preferable to select euploid embryos from mosaic or aneuploid embryos to avoid ongoing aneuploid gestations, if possible. Thus, methods to select embryos before embryo transfer have been investigated, including the use of morphological features, such as polar body shapes, meiotic spindles, vacuoles or refractile bodies, zonae pellucidae, *etc.* However, no features have been decisively established as prognostic value for the further development of oocytes [1]. Furthermore, conventional embryo evaluation using morphological features seemed to be limited in identifying embryos of aneuploidy [2-6]. Some studies have suggested the use of time-lapse parameters for aneuploidy prediction; however, the conclusions are diverging. Generally, researchers concluded that aneuploidy was reflected in cell cycle parameters up to the second day of development, as euploid embryos show more tightly clustered timings than aneuploid embryos do [2,7-9]. It is well-documented, however, that suboptimal embryos may be euploid, and embryos of fine morphological quality might be aneuploid [2,10,11]. Thus, the morphological classification of embryo as euploid or aneuploid has not been established, and the evidence is still weak to validate the introduction of time-lapse assessments in routine conventional clinical settings [2].

Preimplantation genetic testing for aneuploidy [12,13] is an alternative method for investigating chromosomal profiles. Because this method is invasive to the embryo, considerable ethical arguments arise. Thus, the embryo transfer after biopsy is forbidden in some countries. Furthermore, chromosomal profiles might be different at blastocyst sites. The chromosomal profile of a biopsied specimen doesn't always indicate the profile of the rest of the embryo due to genetic heterogeneity. Furthermore, a single trophectoderm biopsy may not represent the complete trophectoderm, as mosaicism in the trophectoderm has been observed [14].

Aneuploidy is known to dramatically increase as women age [15]. Spandorfer (2004) reported that the major underlying cause of increased pregnancy loss with advancing maternal age is chromosomal aneuploidy [16]. Consequently, it is reasonable to presume that methods to predict embryo aneuploidy should incorporate the maternal age. Furthermore, there is currently a demand for a noninvasive method to predict the live birth of a euploid embryo. For these reasons, we explored whether artificial intelligence (AI) could be used to predict a live birth from blastocyst images combined with maternal age data. Deep learning becomes a popular machine learning method [17-25] among methods such as naïve Bayes [26], logistic regression [27], random forest [28], nearest neighbor [29], and neural networks [30]. Thus, in the present pilot study, we had developed an AI classifier using supervised deep learning consisted of a convolutional neural network architecture [31], applied to blastocyst images combined with maternal age data, in an effort to find a noninvasive solution to the selection of embryos that lead to live births. We found that our novel AI classifier using images combined with the maternal age could detect information that conventional embryo evaluation methods could not [20-22].

Zaninovic et al. (2019) reported AI assessment of embryo morphologic features might lend itself to predicting chromosomal integrity [32], but the method was not established for clinical use. Fernandez et al. (2020) demonstrated on their review that there were published papers regarding with AI for reproductive data but there were no reports in terms of aneuploidy of embryos as a desired outcome [33]. Thus, there are no established non-invasive methods to

evaluate aneuploidy of embryos to the best of our knowledge [19]. Then we demonstrate the potential of deep learning to develop a classifier comprised of a neural network to predicting a live birth and an aneuploid miscarriage from the maternal age and an image of the implanted blastocyst.

2. Materials and Methods

2.1. Blastocyst images

Fully de-identified data were used in this study that was approved by the Institutional Review Board at Okayama Couples' Clinic (No. 18000128-04). Patients were provided an explanation of the study and directed to a website with information and an opt-out option.

After blastocyst was formed, an image of the blastocyst was captured approximately 115 hours, or approximately 139 hours after insemination if the blastocyst was not yet large sufficiently. The image was saved on a storage device in JPEG format, without any data that was not able to identify the individual. These de-identified images and maternal age data were input to an off-line system for AI.

A total of 1,586 images of blastocysts which led to live births from 2009 to 2017 and 246 images of blastocysts which led to aneuploid miscarriages from 2008 to 2019, along with maternal age data, were collected. A regression model, with a logistic function applied, was obtained for the ratio of the number of live births to the number of live births plus abortions (*i.e.*, %live births) as a function of maternal age, in the age range at which abortions were observed. Furthermore, because it is well known that maternal age has a strong relationship with aneuploidy, the age distributions were matched, as much as possible, between the live birth and abortion groups. Thus, the age profiles did not differ and the %live births according to maternal age were similar. These matched groups defined the live birth category and abortion category, respectively, used to create the AI classifier. In other words, the live birth category comprised blastocyst images with maternal age data from blastocysts that resulted in a live birth with unknown chromosomal status and the abortion category comprised blastocyst images with maternal age data from blastocysts that resulted in abortion related to chromosomal abnormalities, confirmed by genetic examination of samples of chorionic villus.

2.2. AI Preparation

De-identified images (100×100 pixels), along with maternal age data, were transferred to our AI system. Twenty percent of the images were randomly selected as the test dataset. Among the remaining images, 80% were selected as the training dataset to train the AI classifier, and the rest were the validation dataset. So, these datasets did not overlap. The number of items in the training dataset was augmented, which is often observed in computer science, by rotating the blastocyst image an arbitrary number of degrees to create a new item that were different vector data in the same category.

2.3. AI classifier

We created an original AI classifier using supervised deep learning consisted of a convolutional neural network architecture [30,34], catenated with an elementwise function (*i.e.*, the regression function), to classify blastocyst images combined with the maternal age as either in the abortion category or live birth category, and to acquire the mathematical

probability of being in the live birth category (as well as being in the abnormal category) with L2 regularization [35,36]. (Figure 1)

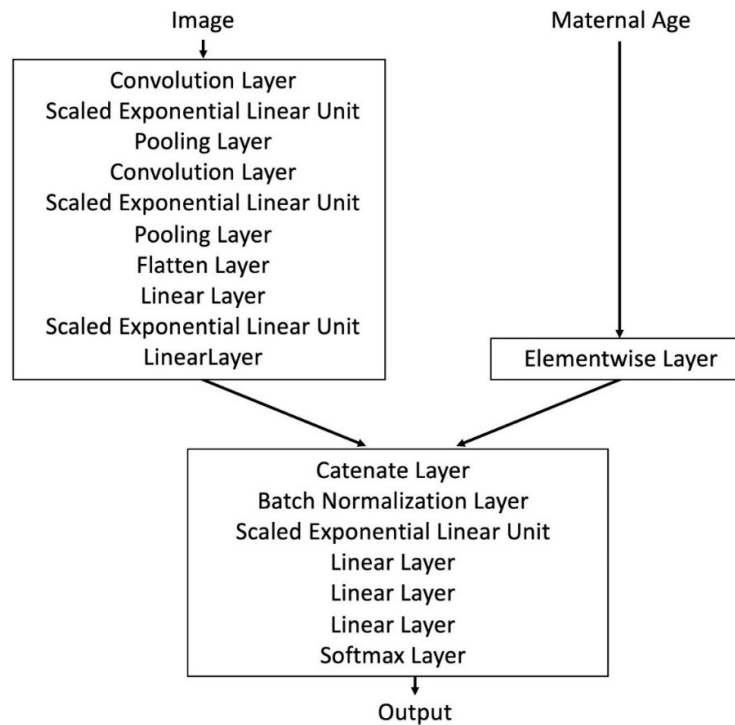


Figure 1: An AI classifier program using supervised deep learning with a convolutional neural network architecture catenated with an elementwise function (the regression function for maternal age) was developed to categorize blastocyst images combined with maternal age data as either in the live birth or abortion category and obtain the mathematical probability of being in the live birth category.

2.4. Developmental environment

The developmental environment used in the present study was as follows: Intel Core i5 processor; 32 GB RAM (Santa Clara, California, USA); nVidia GTX 1080 Ti graphics (Santa Clara, California, USA); Windows (Redmond, Washington, USA); and Wolfram Language 12.0.0 (Wolfram Research, Champaign, IL, USA).

2.5. Statistics

Data are presented as the mean \pm standard deviation (SD), unless otherwise indicated. Statistical analyses were performed using Mathematica 12.0 (Wolfram Research, Champaign, IL, USA). T-tests and logistic regression were carried out. In addition, the accuracy, sensitivity, specificity, positive predictive value and negative predictive value, Youden's J index [37], and the area under the curve (AUC) was used to evaluate the performance of the AI classifier.

3. Results

3.1. Clinical information

Table 1 provides the %live births according to maternal age. The mothers were younger in the live birth group than in the abortion group (33.8 ± 4.25 years versus 37.4 ± 3.96 years,

respectively; $P = 5.07 \times 10^{-31}$ by t-test). The age range in the abortion group was 25 to 44 years old. The logistic regression model for %live births as a function of the maternal age among patients in this age range was as follows: $1 / (1 + \text{Exp}(\beta_0 + \beta_1 x))$, with $\beta_0 = -11.55 \pm 5.36$ ($P=0.03$) and $\beta_1 = 0.28 \pm 0.13$ ($P=0.04$) (estimate coefficient \pm standard error). (Figure 2)

The number of cases in the maternal age-matched live birth and abortion categories were 407 and 246, respectively (Table 2). As expected, the maternal age did not differ between the cases in the live birth and abortion categories (37.17 ± 3.74 years versus 37.35 ± 3.96 years; $P=0.551$). The %live births averaged $60.4\% \pm 5.5\%$, with %live births ranging from 60% to 64% at most of the observed maternal ages (77.8%).

Table 1: Number of abortions and live births, and %live births according to maternal age. The mothers were younger in the live birth group than in abortion group ($P=5.07 \times 10^{-31}$ by t-test).

Maternal age (years)	Abortion, n	Live birth, n	%Live births
20	0	1	100.00%
21	0	0	Not available
22	0	5	100.00%
23	0	3	100.00%
24	0	7	100.00%
25	1	17	94.40%
26	1	27	96.40%
27	4	58	93.50%
28	5	97	95.10%
29	2	67	97.10%
30	0	108	100.00%
31	8	105	92.90%
32	7	147	95.50%
33	8	119	93.70%
34	14	165	92.20%
35	17	129	88.40%
36	26	154	85.60%
37	26	167	86.50%
38	22	139	86.30%
39	24	71	74.70%
40	25	111	81.60%
41	25	69	73.40%
42	15	36	70.60%
>42	16	31	66.00%
Total	246	1587	86.60%

%live births = live births / (live births + abortions)

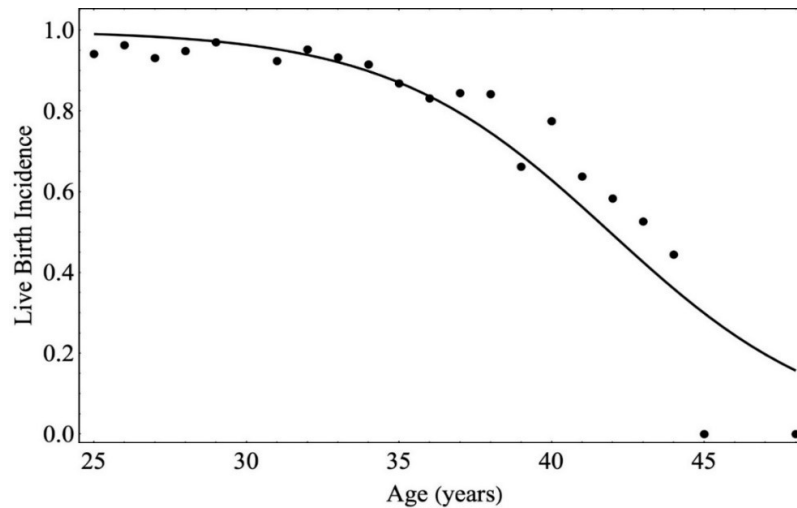


Figure 2: The logistic regression model for the %live birth as a function of the maternal age: $y=1/(1 + \text{Exp}(\beta_0 + \beta_1x))$, with $\beta_0 = -11.55 \pm 5.36$ ($P=0.03$) and $\beta_1 = 0.28 \pm 0.13$ ($P=0.04$) (estimate coefficient \pm standard error).

Table 2: The number of cases in the live birth and abortion categories among the cases matched by maternal age as best as possible. The matched cases in the live birth and abortion categories were used to create the AI classifier. As expected, the mean \pm standard deviation (SD) of the maternal age did not differ between the cases in the live birth and abortion categories (37.17 ± 3.74 years versus 37.35 ± 3.96 years, respectively; $P=0.551$). The mean \pm SD of the %live births was $60.4\% \pm 5.5\%$. For most maternal ages (77.8%) the %live births was between 60% and 64%.

Maternal age (years)	Abortion category, n	Live birth category, n	%Live births
25	1	1	50.00%
26	1	1	50.00%
27	4	7	63.60%
28	5	8	61.50%
29	2	3	60.00%
31	8	14	63.60%
32	7	12	63.20%
33	8	14	63.60%
34	14	24	63.20%
35	17	29	63.00%
36	26	45	63.40%
37	26	45	63.40%
38	22	38	63.30%
39	24	42	63.60%
40	25	44	63.80%
41	25	44	63.80%
42	15	21	58.30%
>42	16	15	46.70%
Total	246	407	62.30%

%live births = live births/(live births + abortions)

3.2. The Best Performing AI Based Model

The best AI classifier was obtained using 1,660 and 424 training data points and validation data points, respectively, and 0.14 as the L2 regularization value. The accuracy, sensitivity, specificity, positive predictive value and negative predictive value, Youden's J index [35], and AUC (mean \pm standard error (SE)) were 0.750, 0.817, 0.640, 0.788, 0.681, 0.457, and 0.730 ± 0.043 , respectively (Table 3; Figure 3). The optimal cutoff point of the receiver operator characteristic curve [38] was 0.623. Classification time by AI was less than 0.20 seconds per case.

Table 3: The results of the best AI classifier using blastocyst images combined with maternal age data from the test dataset (20% of all data points).

Statistic index	AI
Accuracy	0.75
Sensitivity	0.817
Specificity	0.64
positive predictive value	0.788
negative predictive value	0.681
Youden's J index	0.457
AUC (mean \pm standard error)	0.730 ± 0.043

AI: artificial intelligence; AUC: area under the curve

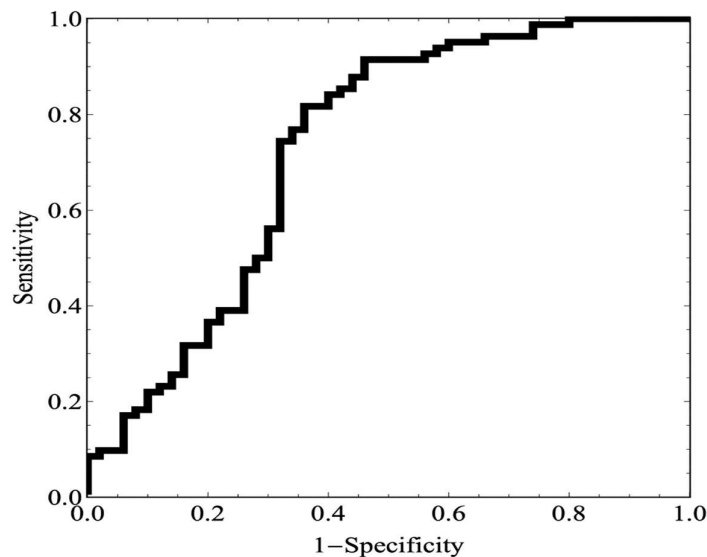


Figure 3: The receiver operator characteristic curve of the AI classifier for predicting a live birth. The area under the curve (AUC) was 0.730 ± 0.043 (mean \pm standard error) and the optimal cutoff point was 0.623.

4. Discussion

In the present study, we made an AI classifier using deep learning consisted of both a convolutional neural network for blastocyst images and elementwise layers for the maternal age. The AI classifier demonstrated an accuracy of 0.750. We previously developed a classifier

using the logistic regression method of machine learning with 80 blastocyst images in each category (live birth and abortion), without maternal age data, and reported its accuracy, sensitivity, specificity, positive predictive value and negative predictive value, Youden's J index and AUC (mean \pm SE) in predicting a live birth as 0.650, 0.600, 0.700, 0.669, 0.638, 0.300, and 0.659 ± 0.043 , respectively [19]. Thus, the AI classifier in the present study is better than our previous classifier, not only in terms of accuracy, but in terms of all statistic indices (*e.g.*, sensitivity and so on). We speculate the following six reasons for the improved accuracy by AI in the present study. First, there were a total of 653 and 160 data points in the present and previous studies, respectively. We consider the larger number of data points in the present study as important in creating an AI classifier with deep learning. Second, AI can use non-image data and image data simultaneously; we consider this advantage of AI as important to improving accuracy. Third, the method used in this study was deep learning consisted of a neural network; in contrast, we used the logistic regression method in our previous study, as it had the best performance among six machine learning methods (neural network, naïve Bayes, logistic regression, random forest, nearest neighbors, and support vector machine). Deep learning seemed to be better for creating an AI classifier for the purpose of selecting embryos. Fourth, using a neural network architecture with a batch normalization layer [39] might be important. We added a batch normalization layer just after concatenating the image and maternal age data. The method draws its strength from rendering normalization and performing normalization for each training mini-batch. We previously reported that this architecture with a batch normalization layer demonstrated good results in classifying squamous epithelial lesions of the uterine cervix from colposcopy images combined with human papilloma virus (HPV) types [17]. Because the dataset in this previous study comprised image and non-image data, it was quite similar to the one in the present study, suggesting that the induction of batch normalization might be useful. We consider this architecture as the fourth reason for the improved accuracy obtained in this study, from the perspective of a neural network architecture with deep learning. Fifth, matching the maternal age between the cases in the live birth and abortion categories for AI input seemed to be appropriate. Older patients have a higher incidence of embryo aneuploidy; thus, we matched the maternal age between the cases in the live birth and abortion categories so that %live births did not substantially differ among maternal ages. In other words, the maternal age factor, thought to be correlated with aneuploidy of the embryo, was stratified by each age. This stratification might be important for data preparation. Sixth, the regression model for the %live births as a function of the maternal age showed a good fit, with $P < 0.05$ for both the estimate coefficient and constant, as shown in (Figure 2). This regression function converted the maternal age values at the elementwise layer in the neural network. We consider it important and useful to discover the appropriate regression function and create the elementwise layer to incorporate this function into the neural network architecture.

There are several reports regarding the accuracy of AI in reproductive medicine. The accuracy for the morphological quality of the blastocyst combined with an evaluation by the embryologist has been reported as 0.98 [40]. Embryos with fair-quality images classified as poor and good quality were 0.509 and 0.614, respectively, for the likelihood of getting a live birth [40]. Furthermore, the accuracy of prediction of a live birth without aneuploidy from a blastocyst image alone was 0.65 [19]. The accuracies of prediction of a live birth from a blastocyst image were 0.64, 0.71, 0.78, 0.81, and 0.88 for the age categories of <35, 35-37, 38-39, 40-41, and ≥ 42 years, and 0.74 for all of ages [20]. The accuracies of AI predicting a live birth by combining a conventional embryo evaluation in patients classified by age were 0.647, 0.675, 0.697, 0.776, and 0.866 for the age categories of <35, 35-37, 38-39, 40-41, and ≥ 42 years, respectively [21]. Some clinical disincentives, such as maternal diseases (*e.g.*, diabetes mellitus [41] and immune disorders [42,43]) impair the ability to achieve a live birth. These factors

cannot be detected by the AI classifier from the maternal age or a blastocyst image. Therefore, statistic indices such as accuracy for a live birth can never reach 1.00. Thus, the accuracy of 0.750 for predicting a live birth in this study seems to be moderately good result for an application of AI in reproductive medicine.

There might be some procedures that could improve the accuracy of AI in predicting embryo aneuploidy. First, clinical information, such as body mass index, complications, and familial genetic profiles, in addition to the maternal age, and/or morphological features obtained in a conventional embryo evaluation, such as inner cell mass grades, might be useful variables for AI with a neural network architecture. However, if the number of variables is too large, the curse of dimensionality [44] occurs, resulting in an inadequate AI classifier. Thus, it is important to select clinical information and/or conventional embryo evaluation variables that have no multicollinearity (*i.e.*, strong correlations among the independent variables) for AI training [17]. Additionally, it might be useful to apply dimension-reduction methods, such as principal component analysis and the variable selection, to reduce dimensionality, if necessary [45]. Second, a large number of data points should be collected, because it is preferable to have more data, rather than less, when exploring scientific questions [46]. Generally, more varied image patterns may be needed, as more than five hundred images might be required in each class for image classification with deep learning [47,48]. When we preliminarily created an AI with a dataset in which the %live births was 50% for all maternal ages (*i.e.*, the numbers of cases in the live birth and abortion categories for each maternal age were same), the statistic indices, such as accuracy were reduced compared to that for the final classifier (data not shown). Thus, the %live births in the present study was not 50%, but averaged about 62.3%, because we tried to use as many images as much as possible, while maintaining the %live births at each maternal age as constant as much as possible. With the addition of more data, especially for the abortion category, the %live births may be set at 50%, which might result in improvements. Third, improvements in the neural network architecture may be possible. The architecture consisted of the neural network for image classification has been proceeding [49-53], but there is no golden standard for creating the architecture. Fourth, the image size is an important issue. The image size for predicting a live birth without aneuploidy from a blastocyst image by machine learning was 100×100 pixels in our previous report [19]. In a colposcopy AI study using images combined with HPV types [17], the accuracy for images of 50×50 pixels were better than one for images of 111×111 or 70×70 pixels. However, images of 15×15 pixels were used to detect cervical cancer [54]. The image size in the present study was 100×100 pixels, and the investigation of other image sizes might be considered. Fifth, regularization values are also one of the important hyperparameters for making a good classifier. Selecting the appropriate number of training and validation data points is also important. Moreover, a validation dataset and the induction of a dropout layer [35], which could prevent overfitting, might be useful in improving the AI classifier.

5. Conclusions

We applied deep learning to develop a classifier comprised of a neural network to predict a live birth from the maternal age and an image of the implanted blastocyst. The classifier predicted a live birth or abortion because of chromosomal abnormalities with an accuracy of 0.75. A complete analysis of each case only required <0.2 seconds. The procedures in this study would not harm the embryo, which can be transferred after acquiring the probability of the prediction. Further study using with more data points and a neural network architecture improvement and hyperparameters may be necessary to validate the classifier. However, the

present study demonstrated the potential of an AI system that might be feasible for clinical practice.

Human rights statements and informed consent

All procedures in this study followed were in accordance with the ethical standards of the responsible committee on human experimentation (institutional and national) and with the Helsinki Declaration of 1964 and its later amendments.

Informed consent was obtained from all of patients for being included in the study.

Furthermore, additional informed consent was obtained from all patients for whom identifying information was included in this article. A website with additional information, including an 'opt-out' option, was set up for this study.

Approval by Ethics Committee

The protocol for the research project, which included human subjects, was approved by the Institutional Review Board at Okayama Couples' Clinic (No. 18000128-04).

References

1. Rienzi L, Vajta G, Ubaldi FM. Predictive value of oocyte morphology in human IVF: a systematic review of the literature. *Hum Reprod Update*. 2011;17:34-45.
2. Kirkegaard K, Ahlström A, Ingerslev HJ, et al. Choosing the best embryo by time lapse versus standard morphology. *Fertil Steril*. 2015;103:323-32.
3. Finn A, Scott L, O'Leary T, et al. Sequential embryo scoring as a predictor of aneuploidy in poor-prognosis patients. *Reprod Biomed Online*. 2010;21:381-90.
4. Eaton JL, Hacker MR, Barrett CB, et al. Influence of patient age on the association between euploidy and day-3 embryo morphology. *Fertil Steril*. 2010;94:365-7.
5. Eaton JL, Hacker MR, Harris D, et al. Assessment of day-3 morphology and euploidy for individual chromosomes in embryos that develop to the blastocyst stage. *Fertil Steril*. 2009;91:2432-6.
6. Wells D. Embryo aneuploidy and the role of morphological and genetic screening. *Reprod Biomed Online*. 2010;21:274-7.
7. Chavez SL, Loewke KE, Han J, et al. Dynamic blastomere behaviour reflects human embryo ploidy by the four-cell stage. *Nat Commun*. 2012;3:1-12.
8. Wong CC, Loewke KE, Bossert NL, et al. Non- invasive imaging of human embryos before embryonic genome activation predicts development to the blastocyst stage. *Nat Biotechnol*. 2010;28:1115-21.

9. Conaghan J, Chen AA, Willman SP, et al. Improving embryo selection using a computer-automated time-lapse image analysis test plus day 3 morphology: results from a prospective multicenter trial. *Fertil Steril*. 2013;100:412.
10. Alfarawati S, Fragouli E, Colls P, et al. The relationship between blastocyst morphology, chromosomal abnormality, and embryo gender. *Fertil Steril*. 2011;95:520-4.
11. Ziebe S, Lundin K, Loft A, et al. FISH analysis for chromosomes 13, 16, 18, 21, 22, X and Y in all blastomeres of IVF pre-embryos from 144 randomly selected donated human oocytes and impact on pre-embryo morphology. *Hum Reprod*. 2003;18:2575-81.
12. Dahdouh EM, Balayla J, Audibert F; Genetics Committee, Wilson RD, Audibert F, et al. Technical update: preimplantation genetic diagnosis and screening. *J Obstet Gynaecol Can*. 2015;37:451-63.
13. Brezina PR, Kutteh WH. Clinical applications of preimplantation genetic testing. *BMJ*. 2015;350:1-12.
14. Gleicher N, Metzger J, Croft G, et al. A single trophoctoderm biopsy at blastocyst stage is mathematically unable to determine embryo ploidy accurately enough for clinical use. *Reprod Biol Endocrinol*. 2017;15:1-8.
15. Chiang T, Schultz RM, Lampson MA. Meiotic origins of maternal age-related aneuploidy. *Biol Reproduct*. 2012;86:1-7.
16. Spandorfer SD, Davis OK, Barmat LI, et al. Relationship between maternal age and aneuploidy in in vitro fertilization pregnancy loss. *Fertil Steril*. 2004;81:1265-9.
17. Miyagi Y, Takehara K, Nagayasu Y, et al. Application of deep learning to the classification of uterine cervical squamous epithelial lesion from colposcopy images combined with HPV types. *Oncol Lett*. 2020;19:1602-10.
18. Miyagi Y, Takehara K, Miyake T. Application of deep learning to the classification of uterine cervical squamous epithelial lesion from colposcopy images. *Mol Clin Oncol*. 2019;11:583-9.
19. Miyagi Y, Habara T, Hirata R, et al. Feasibility of artificial intelligence for predicting live birth without aneuploidy from a blastocyst image. *Reprod Med Biol*. 2019;18:204-11.
20. Miyagi Y, Habara T, Hirata R et al. Feasibility of deep learning for predicting live birth from a blastocyst image in patients classified by age. *Reprod Med Biol*. 2019;18:190-203.
21. Miyagi Y, Habara T, Hirata R, et al. Feasibility of predicting live birth by combining conventional embryo evaluation with artificial intelligence applied to a blastocyst image in patients classified by age. *Reprod Med Biol*. 2019;18:344-56.

22. Miyagi Y, Tada K, Yasuhi I, et al. New method for determining fibrinogen and FDP threshold criteria by artificial intelligence in cases of massive hemorrhage during delivery. *J Obstet Gynaecol Res.* 2020;46:256–65.
23. Miyagi Y, Hata T, Bouno S, et al. Recognition of facial expression of fetuses by artificial intelligence (AI). *J Perinat Med* 2021;49:596-603.
24. Miyagi Y, Hata T, Bouno S, et al. Recognition of fetal facial expressions using artificial intelligence deep learning. *Donald School J Ultrasound Obstet Gynecol* 2021;15:223-8.
25. Miyagi Y, Miyake T. Potential of artificial intelligence for estimating japanese fetal weights. *Acta Med Okayama* 2021;74:483-93.
26. Ben-Bassat M, Klove KL, Weil MH. Sensitivity analysis in Bayesian classification models: multiplicative deviations. *IEEE Trans Pattern Anal Mach Intell.* 1980;3:261-6.
27. Dreiseitl S, Ohno-Machado L. Logistic regression and artificial neural network classification models: a methodology review. *J Biomed Inform.* 2002;35:352-9.
28. Breiman L. Random forests. *Mach Learn.* 2001;45:5-32.
29. Friedman J, Baskett F, Shustek L. An algorithm for finding nearest neighbors. *IEEE Trans Comput.* 1975;24:1000-6.
30. Rumelhart DE, Hinton GE, Williams RJ. Learning representations by back-propagating errors. *Nature.* 1986;323:533-6.
31. Bengio Y, Courville A, Vincent P. Representation learning: a review and new perspectives. *IEEE Trans Pattern Anal Mach Intell.* 2013;35:1798-828.
32. Zaninovic N, Elemento O, Rosenwaks Z. Artificial intelligence: its applications in reproductive medicine and the assisted reproductive technologies. *Fertil Steril* 2019;112:28-30.
33. Fernandez EI, Ferreira AS, Cecilio MHM et al. Artificial intelligence in the IVF laboratory: overview through the application of different types of algorithms for the classification of reproductive data. *J Assist Reprod Genet* 2020;37:2359-76.
34. Schmidhuber J. Deep learning in neural networks: an overview. *Neural Netw.* 2015;61:85-117.
35. Srivastava N, Hinton G, Krizhevsky A, et al. Dropout: a simple way to prevent neural networks from overfitting. *J Mach Learn Res.* 2014;15:1929-58.
36. Nowlan SJ, Hinton GE. Simplifying neural networks by soft weight-sharing. *Neural Comput.* 1992;4:473-93.
37. Youden WJ. Index for rating diagnostic tests. *Cancer.* 1950;3:32-5.
38. Unal I. Defining an optimal cut-point value in ROC analysis: an alternative approach. *Comput Math Methods Med.* 2017;2017:3762651.

39. Ioffe S, Szegedy C. Batch normalization: accelerating deep network training by reducing internal covariate shift. arXiv. 2015;37:448-56.
40. Khosravi P, Kazemi E, Zhan Q, et al. Robust automated assessment of human blastocyst quality using deep learning. bioRxiv 2018;1-24.
41. Ota K, Ohta H, Yamagishi S. Diabetes and female sterility/infertility: diabetes and aging-related complications. (1stedn) Springer, Singapore. 2018.
42. Practice Committee of the American Society for Reproductive Medicine. The role of immunotherapy in in vitro fertilization: a guideline. Fertil Steril. 2018;110:387-400.
43. Hong YH, Kim SJ, Moon KY, et al. Impact of presence of antiphospholipid antibodies on in vitro fertilization outcome. Obstet Gynecol Sci. 2018;61:359-66.
44. Bellman RE. Adaptive control processes: a guided tour. Princeton University Press, Princeton, New Jersey. 1961;pp.255
45. Lever J, Krzywinski M, Altman N. Points of Significance: Model selection and overfitting. Nat Methods. 2016;13:703-4.
46. Altman N, Krzywinski M. The curse(s) of dimensionality. Nat Methods. 2018;15:397-400.
47. Sato M, Horie K, Hara A, et al. Application of deep learning to the classification of images from colposcopy. Oncol Lett. 2018;15:3518-23.
48. Esteva A, Kuprel B, Novoa RA, et al. Dermatologist-level classification of skin cancer with deep neural networks. Nature. 2017;542:115-8.
49. Krizhevsky A, Sutskever I, Hinton GE. Imagenet classification with deep convolutional neural networks. In: Pereira F, Burges CJC, Bottou L Weinberger KQ (eds). Advances in neural information processing systems 25. NY, USA: Curran Associates, Inc.2012; pp.1097-1105.
50. Simonyan K, Zisserman A. Very deep convolutional networks for large-scale image recognition. 3rd International CLR meeting, USA. 2015.
51. Szegedy C, Liu W, Jia Y, et al. Going deeper with convolutions. Proceedings of the IEEE Conference on CVPR, Boston. 2015.
52. He K, Zhang X, Ren S, et al. Deep residual learning for image recognition. AeXiv e-prints. 2015;6:1-12.
53. Hu J, Shen L, Albanie S, et al. Squeeze-and-excitation networks. IEEE Trans Pattern Anal Mach Intell 2019;42:2011-23.
54. Kudva V, Prasad K, Guruvare S. Automation of detection of cervical cancer using convolutional neural networks. Crit Rev Biomed Eng. 2018;46:135-45.